COBEM 2021 26th International Congress of Mechanical Engineering
November 22-26, 2021, Virtual Congress, Brazil
ABCM Associação Brasileira de Engenharia e Ciências Mecânicas

COB-2021-2041
TWO-DIMENSIONAL CFD ANALYSIS OF THE H-DARRIEUS WIND TURBINE USING OPENFOAM

Arthur Leite Guilherme
Universidade de Brasília - Brasília - Federal District - Brasil - CEP: 70910-900.
arthur.guilherme@aluno.unb.br

Gilberto A. A. Moreira
João Alves Lima
Universidade Federal da Paraíba, Cidade Universitária - João Pessoa - PB - Brasil - CEP: 58051-970.
gilberto@cear.ufpb.br
jalima@cear.ufpb.br

Abstract. *The pressure to implement clean and renewable energy in the energy matrix due to the global warming threat, the improved energy security promoted by decentralized generation and the desire of smart cities intensified research in wind energy solutions for urban environments in the last few decades. In this context, the Vertical Axis Wind Turbines (VAWT) have advantages over horizontal axis turbines because they do not need alignment with the wind direction and because they have heavy machinery attached to the ground. In order to contribute to this research area, this work aims to apply and evaluate a two-dimensional Computational Fluid Dynamics approach to the transient simulation of a wind turbine type H-Darrieus. The URANS approach with the SST k-omega turbulence model for the closure problem in a hybrid mesh with a rotating part was used in this work with the OpenFOAM library. The power coefficient in function of the blade tip speed ratio λ and the wake characteristics numerically obtained were compared to experimental data available in the literature. The numerical results showed, despite the simplification of the two-dimensional model, good agreement with the experimental results with regard to the shape of the power coefficient curve and the characteristics of the wake, reinforcing the efficiency of the computational modeling performed with OpenFOAM.*

Keywords: *H-Darrieus, Wind Power, CFD, OpenFOAM, URANS.*

1. INTRODUCTION

Amid the threat of global warming due to the burning of fossil fuels and the desire of a more reliable energy matrix that could be achieved with decentralized power production, the research in sustainable energy solutions for urban environments has been increasing in the last few decades. Unlike the photovoltaic technology (PV), the wind solutions still are incipient in micro-generation technologies, achieving only 2,66% of the energy produced by PV in Brazil in this category (EPE, 2019).

In the context of micro-generation, especially in urban environment, the VAWTs have advantages over the HAWTs (Horizontal Axis Wind Turbines) because they do not need alignment with the wind direction, which is very intermittent, and they have heavy machinery attached to the ground.

However the VAWTs have advantages over the HAWTs in the urban environment, there are not consolidated methodologies to predict the power performance of VAWTs as there are with HAWTs. This work aims to contribute with this research area by applying and evaluate a two-dimensional Computational Fluid Dynamics (CFD) approach on simulating and thus predicting the performance of a H-Darrieus type of VAWT. The model was compared to the experimental work of (Battisti *et al.*, 2018).

The following section introduce some used methodologies and relevant geometric and operational parameters of H-Darrieus wind turbines. Section 3shows the applied numerical model in this work. In Section 4we present the obtained results and discussion and in Section 5we make our conclusions.

2. H-DARRIEUS TURBINE

2.1 H-Darrieus dynamics

The H-Darrieus is a lift driven type wind turbine. Therefore, the major force that contributes with the generation of torque at the shaft is the lift felt by the blades. Yet, differently of HAWTs, the plan of rotation is parallel to the stream

direction, which makes its dynamics very complex.

The aerodynamic performanc of a VAWT can be defined as the power coefficient (C_P), given by:

$$C_p = \frac{T\lambda}{\frac{1}{2}\rho A_r R V_\infty^2} \tag{1}$$

Where *T* is the total torque, λ is the tip speed ratio, A_r is the sweep area, *R* is the rotor radius and V_∞ is the free stream velocity.

The main parameters that influence the aerodynamic performance (C_p) of a VAWT, in general, and a H-Darrieus, in particular, are Gosselin *et al.* (2016); Rezaeiha *et al.* (2018a):

- Geometric parameters: Blade profile and chord (c), number of blades (*N*), solidity (σ), aspect ratio (*AR*), blade roughness, connection arms and presence and shape of end plates;
- Operational parameters: tip speed ratio (λ), Reynolds number and turbulence intensity.

The manner in which these parameters influence in the extracted power has been extensively studied in recent decades. The solidity, one of the most important, was studied by (Sabaeifard *et al.*, 2012), who observed the peak of curve C_p shifts to higher λ with increasing solidity. The aspect ratio was studied by (Gosselin *et al.*, 2016) and (Du *et al.*, 2019), who concluded that longer blade lengths and the consequent increase in *AR* reduce blade tip losses caused by the 3D effect, thus increasing efficiency. Du *et al.* (2019) also studied blade wall roughness and different blade profiles. With respect to profile, the author concluded that some profiles have bigger peaks of efficiency and others have better self-initialization properties.

2.2 H-Darrieus Performance

There are different methods to study the performance of the H-Darrieus turbine. Based on a literature review, Jin *et al.* (2015) divided them into three main types: (1) experimental methods, (2) computational aerodynamics, and (3) computational fluid dynamics.

Among the experimental methods, the two most important are wind tunnel experiments with speed, pressure and torque sensors indicated to measure the power performance and PIV (Particle Image Velocimetry), which is indicated to analyse wake characteristics.

The computational aerodynamics methods use the theories of aerodynamics in their models. According to Islam *et al.* (2008), they can be divided in three categories: momentum-based models, vortex models and cascade models.

Computational fluid dynamics, used in this work, uses the conservation laws in a discretized 2D or 3D domain. This method has been more used in recent years due to the increase in computational capacity of the computers. Although it has a computational cost significantly higher than the aerodynamic models it is able to simulate and visualize the flow in details. The *URANS* model, i.e., the unsteady approach of the Reynolds Averaged Navier-Stokes equations was used in this work. The chosen turbulence closure model was the SST k-ω.

3. NUMERICAL MODELLING

3.1 Geometry and mesh

The geometry was based on the rotor used in the experimental work of Battisti *et al.* (2018), Fig. 1, which will serve as basis of validation and evaluation of the performance of the model used in this work. Table 1 presents the main characteristics.

Table 1: Rotor geometric characteristics

R [m]	**c [m]**	**Profile**	**N [-]**	σ	**AR [-]**	$\mathbf{A_r}$ $[\mathbf{m^2}]$
0.514	0.085	NACA0021	3	0.25	17.18	1.5

The NACA 0021 profile was generated from the parametric equations Eq. (2) and (3) with $c = 0.085m$. However, this formula do not provide connection between the top and bottom of the blade, requiring an approach to link them. In order to facilitate generation of the viscous sublayer mesh, a rounded trailing edge was employed, as sketched in Fig. 2.

$$y = 5ec(0.2969\sqrt{t} - 0.1260t - 0.3516t^2 + 0.2843t^3 - 0.1015t^4) \tag{2}$$

$$x = ct \tag{3}$$

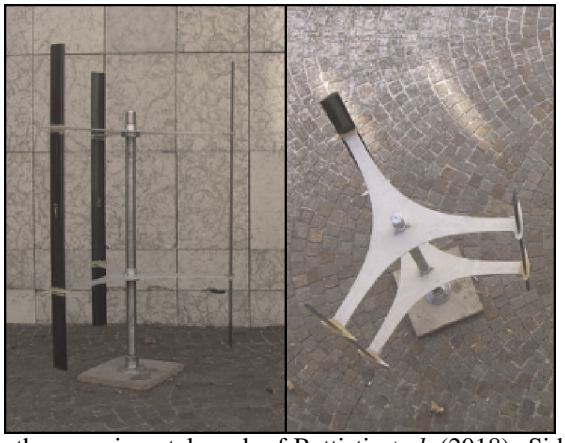

Figure 1: H-Darrieus rotor used in the experimental work of Battisti *et al.* (2018). Side view (left) and top view (right). Adapted from: (Battisti *et al.*, 2018). A_r is the sweep area.

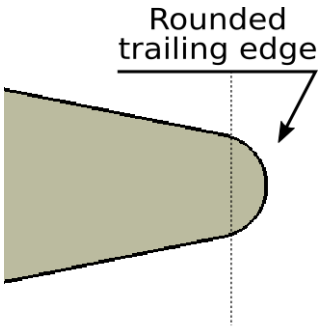

Figure 2: Rounded trailing edge.

Where (x, y) represents the coordinates of the half blade, c the chord lenght, e the maximum thickness ratio and $t \in (0, 1)$ the fraction of traversed chord.

The blade-arm connection point was not explained in the experimental work, so it was chosen to be at the middle of chord ($0.5c$). The cylindrical shaft of $0.05m$ was included in the 2D domain in order to capture its wake effect. The decision of the size of the computational domain was made based on the guidelines provided by the systematic analysis of (Rezaeiha *et al.*, 2018b). According to the authors, a distance of $30R$ between the inlet and the center of the rotor is enough, so that the induction field upstream of the turbine, characterized by the deceleration of the flow, is completely contained within the computational domain and, thus, does not influence the performance prediction. Also, following the guidelines, a domain width of $80R$ was adopted, double the recommended minimum to obtain a blockage correction factor less than 5%. A distance from the center of the rotor to the outlet of $110R$ was chosen to guarantee a fully developed flow. Figure (3) shows the adopted computational domain.

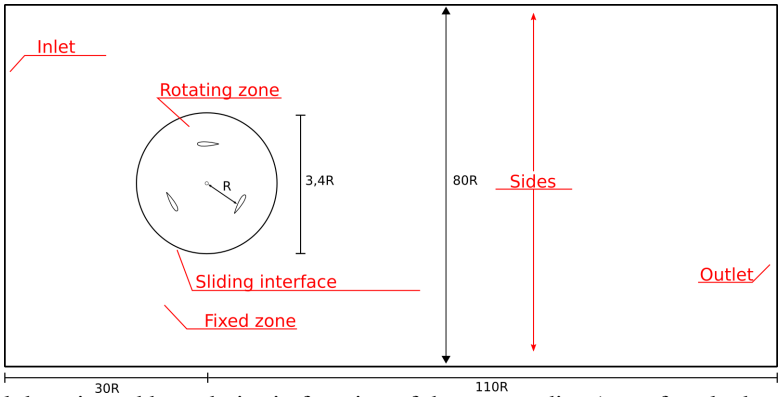

Figure 3: Computational domain and boundaries in function of the rotor radius (out-of-scale drawing). Elaborated by the author.

As can be seen in Fig. (3), was divided into a fixed and a rotating zone. To the last is applied a constant rotation velocity, see Section 3.2Its radius is about 1.7 times the rotor radius.

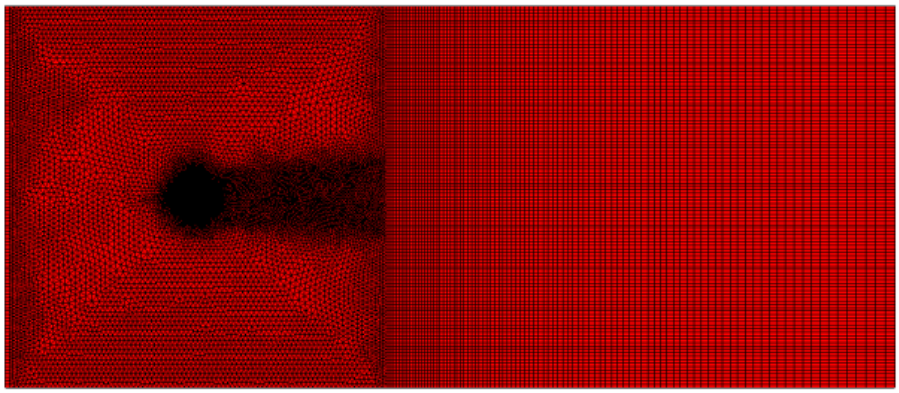

(a) Full domain

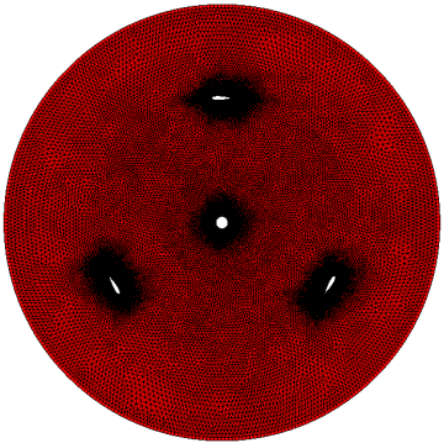

(b) Rotating zone

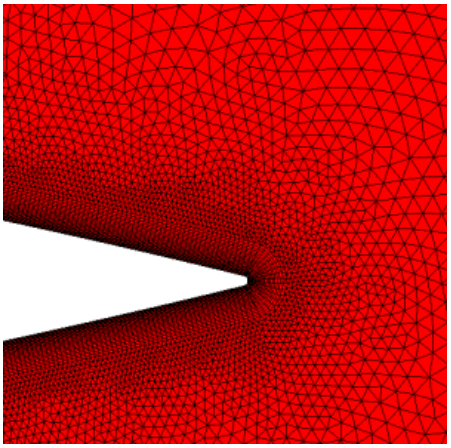

(c) Near the blade trailing edge

Figure 4: Hybrid mesh.

3.2 Boundary conditions

In order to approximate the conditions carried out in the experimental work Battisti *et al.* (2018), a constant rotation equivalent to $400rpm$ was applied to the rotating zone in all simulations, while the velocity at the inlet was changed for each case. The sliding interface that separates the fixed and rotating zones was used using AMI (*Arbitrary Mesh Interface*), which allows the coupling of adjacent and disconnected zones, assigning to each face a weighted contribution according to the portions of the partially overlapping faces of the neighboring zone. In a rotating mesh, it allows the faces to not need to be well matched and thus not need a time step strictly equal to the cell size divided by the rotation speed. In OpenFOAM©, the boundary condition *cyclicAMI* implements this condition.

Fixed velocity conditions with turbulence intensity (*TI*) of 1% were applied at the inlet (highest value found upstream of the turbine in the experimental work). The turbulence model used was the $k-\omega$ *SST*. Thus, the boundary conditions of the turbulent kinetic energy k_c and the specific dissipation rate of turbulent kinetic energy ω_c at the input were, respectively, *turbulentIntensityKineticEnergyInlet* and *turbulentMixingLengthFrequencyInlet*, which provide values according to Eq. (4) e (5), where L is the turbulence length scale chosen to be 15% of the rotor diameter and C_μ a model constant equal to 0.09.

$$k_c = 1,5(IT|V_\infty|)^2 \tag{4}$$

$$\omega_c = \frac{k_c^{0,5}}{C_\mu^{0,25} L} \tag{5}$$

The conditions of fixed pressure at the outlet and symmetry on the sides of the domain were used, which are good approximations for a sufficiently large domain in the transverse and longitudinal directions. In the blades and cylindrical shaft (walls), the wall functions *nutUSpaldingWallFunction* for turbulent viscosity ν_t and *omegaWallFunction* for specific dissipation rate were used. For k_c, a fixed value of $10^{-10}\ m^2/s^2$ has been set. Details of the implementation in OpenFOAM© of the aforementioned wall functions can be found in (Liu, 2016).

The air kinematic viscosity ν, in turn, was configured in the *transportProperties* dictionary according to the operating temperature of each case (explained in the experimental work).

Table 2 summarize the adopted boundary conditions.

Table 2: Resumo das condições de contorno por contorno ou zona.

Boundary/Zone	**Boundary Conditions**
Rotating zone	• Angular velocity of 400 rpm
Sliding interface	• *cyclicAMI*
Inlet	• V_∞: 9 a 12 m/s • Turbulence intensity: 1% • Turbulence length scale: 15% of the rotor diameter
Outlet	• Fixed pressure: 0 m^2/s^2 • Homogeneous Neumann condition to the other variables. In OpenFOAM©: *zeroGradient*
Walls	• Wall functions *nutUSpaldingWallFunction* for turbulence viscosity and *omegaWallFunction* for ω_c • Turbulent kinetic energy: 1e-10 m^2/s^2
Sides	• Symmetry condition

3.3 Numerical settings

The solver used was *pimpleFoam* which uses the PIMPLE algorithm (combination of PISO and SIMPLE) to solve transient problems of incompressible and turbulent flows. This solver allows the use of dynamic meshes with moving bodies, which is the case of these simulations. A maximum of 40 iterations per time step was chosen with 2 pressure corrections. This high number of iterations increases the runtime, nevertheless it makes the algorithm more robust, enabling stability with Courant number $Co > 1$ (Holzmann, 2017). Therefore, it was used a adaptive time step approach with maximum $Co = 8$.

As for the numerical schemes, at the beginning of the simulations, first order schemes were used in the computing of gradients and in time in order to guarantee stability, namely *Linear Gauss* and *Euler*. Later in the simulations, these schemes were replaced by second order ones in order to improve accuracy: *leastSquares* and *CrankNicolson*, respectively.

The percentage deviation of the mean C_p between two subsequent revolutions was used as a convergence criterion, which is a common practice in the simulations of H-Darrieus (Balduzzi *et al.*, 2016). Although the study of Balduzzi *et al.* (2016) showed that the value of 1% is not enough for a true convergence, thus suggesting a value of 0.1%, the criterion with 1% was used in this work to save time, Eq. (6).

$$\frac{\overline{C_{p_n}} - \overline{C_{p_{n-1}}}}{\overline{C_{p_{n-1}}}} 100\% < 1\% \tag{6}$$

Where the subscript refers to the *nth* revolution.

4. RESULTS AND DISCUSSION

Figure 5 shows C_p as a function of λ obtained numerically in comparison with those obtained in the experimental work of Battisti *et al.* (2018). The results show a high overestimation of the power coefficient obtained by the two-dimensional analysis, reaching an increase of almost 50% for the optimal λ.

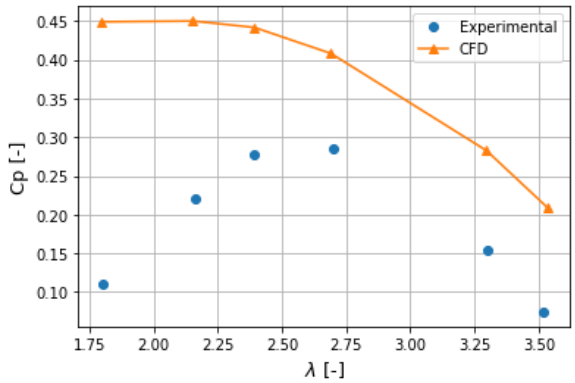

Figure 5: Power coefficient curves obtained numerically (this work) and experimentally (Battisti *et al.*, 2018).

Similar overestimation in 2D CFD analyzes were also found by other authors, reaching a predicted coefficient up to 70% higher than that found experimentally for optimal λ (Howell *et al.*, 2010; Castelli *et al.*, 2011; Gosselin *et al.*, 2016). This greater performance of the two-dimensional model is possibly due to the failure to take into account the losses caused by the three-dimensional effect of blade tip vortices and the parasitic torque caused by the wind drag on the rotor structures (connection arms, screws, etc.) (Castelli *et al.*, 2010).

For $\lambda \leq 2.39$, however, additional numerical effects may have generated a worse performance in the estimation of C_p causing a shift of the maximum point to the left and causing the curve not to decay as expected.

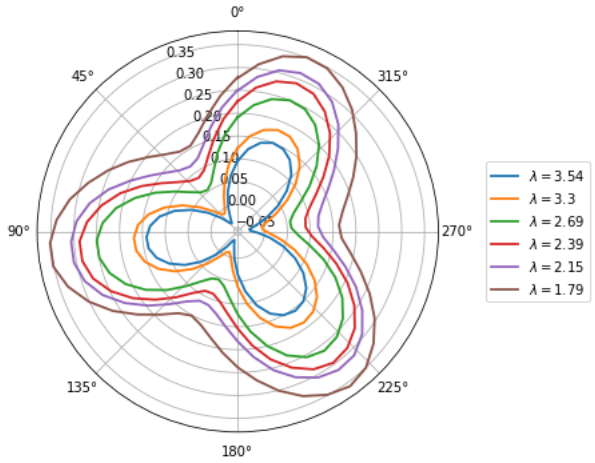

Figure 6: Instantaneous torque coefficient on the rotor as a function of the azimuth angle.

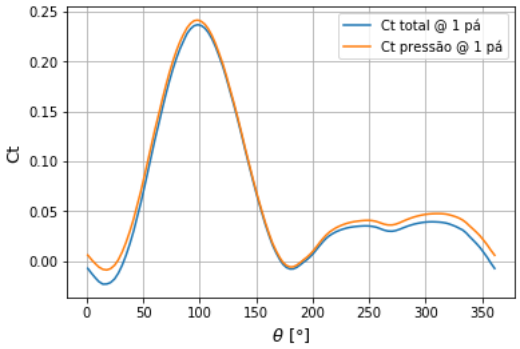

Figure 7: Instantaneous torque coefficient as a function of azimuthal angle for one blade with shear forces included (C_T total) and not included (C_T pressure) for $\lambda = 2.4$

The analysis of the instantaneous torque coefficient C_T along one revolution, Fig. (6), reveals that the azimuthal position where the greatest torque is provided to the blade is around $\theta = 100°$, for all tested λ. The minima points, in turn, occur when one of the blades approaches $\theta = 45°$ for $\lambda = 3.54$ and they tend to advance the smaller the λ is.

Figure 7 also shows the negative contribution of shear forces to torque generation, since the total torque (pressure and shear forces) always remains lower than the torque provided only by the pressure forces, standing out at θ close to $0°$, when the blade receives the wind almost frontally, with small angles of attack.

With regard to the turbine wake, Fig. (8) shows the comparison between the results of the mean velocity deficit over one complete revolution. The profiles are taken at three times the radius of the rotor ($3R$) with respect to the center of the rotor. Fig. (9), in turn, shows the normalized velocity field for $\lambda = 2.4$.

Observing the numerical results, it can be seen that the wind, when passing through the turbine, suffers a drastic reduction in its speed, reaching a reduction of 75% for $\lambda = 3.3$. This reduction is smaller the smaller λ is, with a reduction around 55% for $\lambda = 1.8$. Also, it is possible to see a reduction in the wake width the smaller λ is.

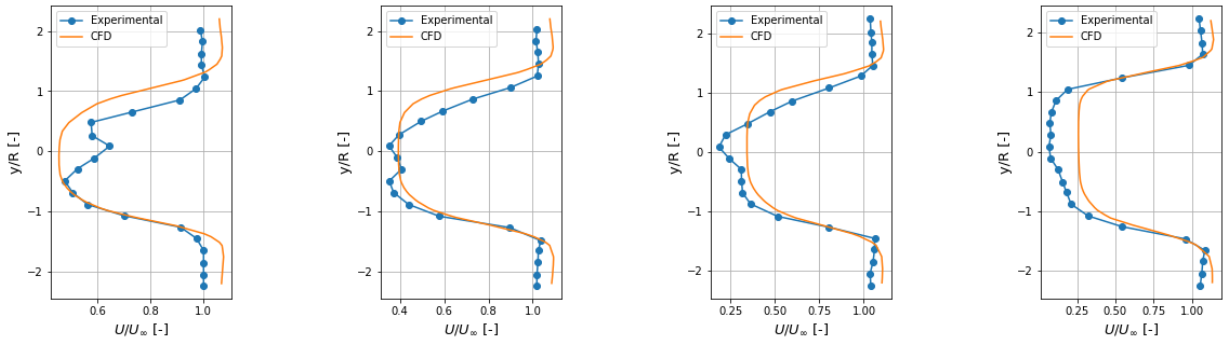

(a) $\lambda = 1.8$ (b) $\lambda = 2.16$ (c) $\lambda = 2.4$ (d) $\lambda = 3.3$

Figure 8: Mean velocity deficit at x = 3R. Comparison between numerical (this work) and experimental (Battisti *et al.*, 2018) results.

Although the numerical results indicate reliably the expected deficit range, they fail to capture the peaks caused by the instability of the wake.

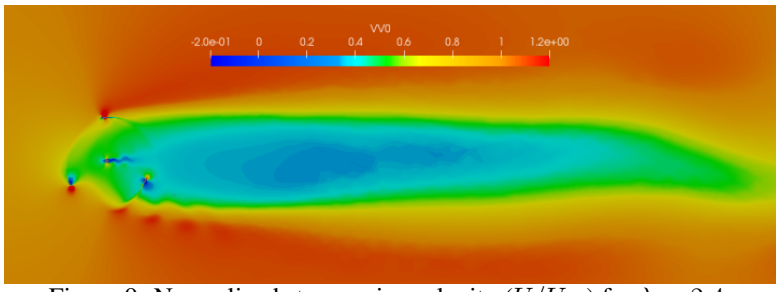

Figure 9: Normalized streamwise velocity (U/U_∞) for $\lambda = 2.4$.

Fig. (10) shows the turbulence intensity present in the wake at $x = 3R$. It can be observed a good prediction of the 2D model, which denotes turbulence intensity peaks close to $y/R \approx \pm 1$ similar to those obtained in the experimental work. However, a different trend is noticed with the increase of λ, where the experiments indicated a tendency to decrease in intensity, while the simulation resulted in the opposite trend.

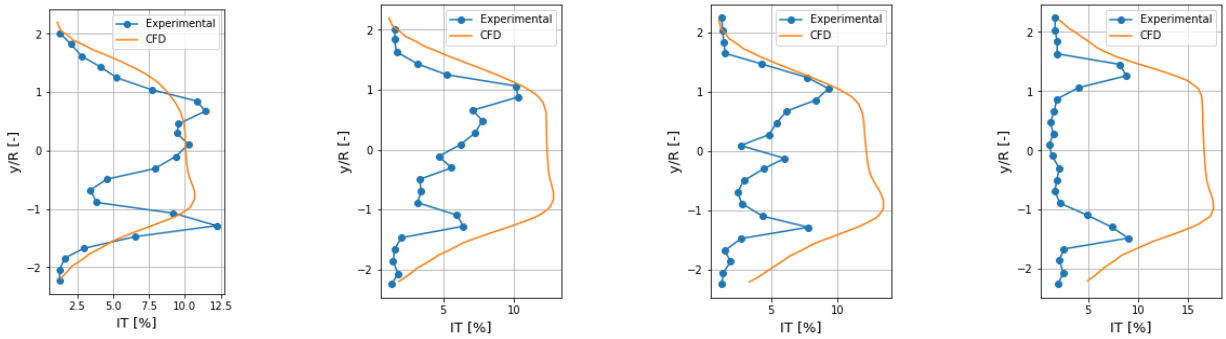

(a) $\lambda = 1.8$ (b) $\lambda = 2.16$ (c) $\lambda = 2.4$ (d) $\lambda = 3.3$

Figure 10: Turbulence intensity at x = 3R. Comparison between numerical (this work) and experimental (Battisti *et al.*, 2018) results.

5. CONCLUSIONS

The two-dimensional model of the H-Darrieus turbine using OpenFOAM© developed in this work proved to be suitable for turbine performance and wake analysis. However, the model overestimated the coefficient of performance, where the largest deviation, when compared to the experimental one, occurred at low blade tip speed ratios, where the formation of dynamic stall is likely to happen with more intensity, indicating a difficulty of the model in capturing this phenomenon. In general, the overvalued performance can be attributed to not considering three-dimensional effects that generate losses to the system, such as vortices at the tips of the blades and the parasitic torque that arises in the rotor

structures. To overcome this problem is suggested to future works the add to the model an semi-empiric estimate of the parasitic torque on the struts, as well as the implementation of turbulence transition models.

6. ACKNOWLEDGEMENTS

The authors thank the CNPQ for the resources and the maintenance of the scholarship to the student.

7. REFERENCES

Balduzzi, F., Bianchini, A., Maleci, R., Ferrara, G. and Ferrari, L., 2016. "Critical issues in the CFD simulation of Darrieus wind turbines". *Renewable Energy*, Vol. 85, pp. 419–435. doi:10.1016/j.renene.2015.06.048.

Battisti, L., Persico, G., Dossena, V., Paradiso, B., Raciti Castelli, M., Brighenti, A. and Benini, E., 2018. "Experimental benchmark data for H-shaped and troposkien VAWT architectures". *Renewable Energy*, Vol. 125, pp. 425–444. doi: 10.1016/j.renene.2018.02.098.

Castelli, M.R., Ardizzon, G., Battisti, L., Benini, E. and Pavesi, G., 2010. "Modeling strategy and numerical validation for a Darrieus vertical axis micro-wind turbine". *ASME International Mechanical Engineering Congress and Exposition, Proceedings (IMECE)*, Vol. 7, No. PARTS A AND B, pp. 409–418. doi:10.1115/IMECE2010-39548.

Castelli, M.R., Englaro, A. and Benini, E., 2011. "The Darrieus wind turbine: Proposal for a new performance prediction model based on CFD". *Energy*, Vol. 36, No. 8, pp. 4919–4934. doi:10.1016/j.energy.2011.05.036.

Du, L., Ingram, G. and Dominy, R.G., 2019. "Experimental study of the effects of turbine solidity, blade profile, pitch angle, surface roughness, and aspect ratio on the H-Darrieus wind turbine self-starting and overall performance". *Energy Science & Engineering*, Vol. 7, No. 6, pp. 2421–2436. doi:10.1002/ese3.430.

EPE, E.d.P.E., 2019. "Brazilian Energy Balance 2019 Year 2018". Technical report.

Gosselin, R., Dumas, G. and Boudreau, M., 2016. "Parametric study of H-Darrieus vertical-axis turbines using CFD simulations". *Journal of Renewable and Sustainable Energy*, Vol. 8, No. 5. doi:10.1063/1.4963240.

Holzmann, T., 2017. "Mathematics, Numerics, Derivations and OpenFOAM". *Configurable Distributed Systems, 1992., International Workshop on*, , No. July, pp. 68–79. doi:10.13140/RG.2.2.27193.36960.

Howell, R., Qin, N., Edwards, J. and Durrani, N., 2010. "Wind tunnel and numerical study of a small vertical axis wind turbine". *Renewable Energy*, Vol. 35, No. 2, pp. 412–422. doi:10.1016/j.renene.2009.07.025.

Islam, M., Ting, D.S. and Fartaj, A., 2008. "Aerodynamic models for Darrieus-type straight-bladed vertical axis wind turbines". *Renewable and Sustainable Energy Reviews*, Vol. 12, No. 4, pp. 1087–1109. doi:10.1016/j.rser.2006.10.023.

Jin, X., Zhao, G., Gao, K. and Ju, W., 2015. "Darrieus vertical axis wind turbine: Basic research methods". *Renewable and Sustainable Energy Reviews*, Vol. 42, pp. 212–225. doi:10.1016/j.rser.2014.10.021.

Liu, F., 2016. "A Thorough Description Of How Wall Functions Are Implemented In OpenFOAM". *CFD With Open-Source Software, edited by Nilsson H.* URL `http://www.tfd.chalmers.se/ hani/kurser/OS_CFD_2016`.

Rezaeiha, A., Montazeri, H. and Blocken, B., 2018a. "Characterization of aerodynamic performance of vertical axis wind turbines: Impact of operational parameters". *Energy Conversion and Management*, Vol. 169, No. May, pp. 45–77. doi:10.1016/j.enconman.2018.05.042.

Rezaeiha, A., Montazeri, H. and Blocken, B., 2018b. "Towards accurate CFD simulations of vertical axis wind turbines at different tip speed ratios and solidities: Guidelines for azimuthal increment, domain size and convergence". *Energy Conversion and Management*, Vol. 156, No. September 2017, pp. 301–316. doi:10.1016/j.enconman.2017.11.026.

Sabaeifard, P., Razzaghi, H. and Forouzandeh, A., 2012. "Determination of Vertical Axis Wind Turbines Optimal Configuration through CFD Simulations". *2012 International Conference on Future Environment and Energy*, Vol. 28, pp. 109–113.

8. RESPONSIBILITY NOTICE

The authors are solely responsible for the printed material included in this paper.